*Inorg. Chem.* **2005**, *44*, 2908–2919


# Conformations, Protonation Sites, and Metal Complexation of Benzohydroxamic Acid. A Theoretical and Experimental Study

**Begoña García,*,† Saturnino Ibeas,† José M. Leal,† Fernando Secco,*,‡ Marcella Venturini,‡ Maria L. Senent,§ Alfonso Niño,|| and Camelia Muñoz||**

*Departamento de Química, Universidad de Burgos, 09001 Burgos, Spain, Dipartimento di Chimica e Chimica Industriale, Università di Pisa, 56126 Pisa, Italy, Departamento de Astrofísica Molecular e Infrarroja, Instituto de Estructura de la Materia, Consejo Superior de Investigaciones Científicas, 28006 Madrid, Spain, and Escuela Superior de Informática, Universidad de Castilla la Mancha, 13071 Ciudad Real, Spain*

Received April 30, 2004

A theoretical and experimental study on the structure and deprotonation of benzohydroxamic acid (BHA) has been performed. Calculations at the RHF/cc-pVDZ level, refined by the B3LYP/AUG-cc-pVDZ method, indicate that, in the gas phase, *Z* amide is the most stable structure of both neutral and deprotonated BHA. $^1$H–$^1$H nuclear Overhauser enhancement spectroscopy and $^1$H–$^1$H correlation spectroscopy spectra in acetone, interpreted with ab initio interatomic distances, reveal that BHA is split into the *Z* and *E* forms, the [*E*]/[*Z*] ratio being 75:25 at –80 °C. The formation of *E*–*E*, *Z*–*Z*, and *E*–*Z* dimers has been detected; in the presence of water, the dimers dissociate to the corresponding monomers. The rates of proton exchange within the *Z* and *E* forms and between *E* and *Z* were measured by dynamic $^1$H NMR in the –60 to 40 °C temperature range; an increase in water content lowers the rate of exchange of the *E* isomer. The effect of $D_2O$ on the NMR signals indicates a fast hydrogen exchange between $D_2O$ and the *E* and *Z* amide forms. The sequence of the acid strength at low temperatures is $(N)H_E \approx (O)H_E < (O)H_Z \approx (N)H_Z$. The kinetics of complex formation between BHA and $Ni^{2+}$, investigated by the stopped-flow method, show that both neutral BHA and its anion can bind $Ni^{2+}$. Whereas the anion reacts at a "normal" speed, the rate of water replacement from $Ni(H_2O)_6^{2+}$ by neutral BHA is about 1 order of magnitude less than expected. This behavior was interpreted assuming that, in aqueous solution, BHA mainly adopts a closed (hydrogen-bonded) *Z* configuration, which should open (with an energy penalty) for the metal binding process to occur.

## Introduction

Hydroxamic acids are useful reagents for biological, medical, and industrial applications;[1] particularly interesting is their ability to form stable chelates with metal ions. Despite the effort devoted to elucidate their behavior, hydroxamic acids remain poorly characterized; in fact, a reliable assignment of the correct structure is challenging because the several possible conformations strongly depend on concentration, temperature, and the nature of the solvent.[2] Earlier theoretical and NMR studies showed that certain hydroxamic acids may adopt either the *Z* (cis) or *E* (trans) conformation, separated by a high energy barrier;[3,4] moreover, amide/imide tautomerism has been postulated for the *Z* and *E* isomers;[3,5] hence, a general hydroxamic acid RCONHOH is prone to four different forms (Scheme 1). On the basis of theoretical calculations and by analogy with amides,[6] some authors concluded that the *Z* form becomes stabilized by either

* Authors to whom correspondence should be addressed. Tel: +34 947 258819. Fax: +34 947 258831. E-mail: begar@ubu.es (B.G.). Tel.: +39 050 2219259. Fax: +39 050 2219260. E-mail: ferdi@dcci.unipi.it (F.S.).
† Universidad de Burgos.
‡ Università di Pisa.
§ Consejo Superior de Investigaciones Científicas.
|| Universidad de Castilla la Mancha.

(1) Bauer, L.; Exner, O. *Angew. Chem., Int. Ed. Engl.* **1974**, *13*, 376−384.
(2) García, B.; Ibeas, S.; Muñoz, A.; Leal, J. M.; Ghinami, C.; Secco, F.; Venturini, M. *Inorg. Chem.* **2003**, *42*, 5434−5441.
(3) Senent, M. L.; Niño, A.; Muñoz-Caro, A.; Ibeas, S.; García, B.; Leal, J. M.; Secco, F.; Venturini, M. *J. Org. Chem.* **2003**, *68*, 6535−6542.
(4) (a) Brown, D. A.; Glass, W. K.; Mageswaran, R.; Girmany, B. *Magn. Reson. Chem.* **1988**, *26*, 970−973. (b) Caudle, M. T.; Crumbliss, A. L. *Inorg. Chem.* **1994**, *33*, 4077−4085.



10.1021/ic049438g CCC: $30.25 
Published on Web 03/17/2005

**Scheme 1**

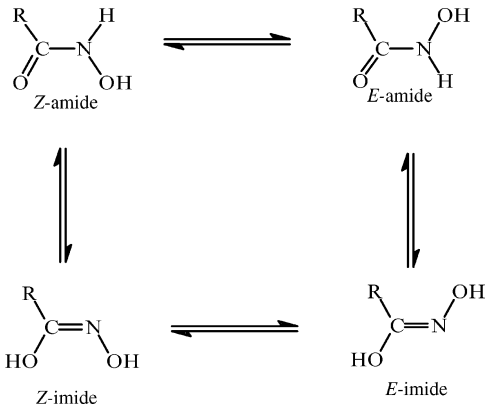


intramolecular (nonpolar solvents)[7] or intermolecular (protic solvents) H bonding.[8] Concerning substituted hydroxamic acids (RCONR′OH), our results with N-phenyl-BHA have shown that the *E* isomer prevails in acetone and the *Z* isomer in water, whereas in methanol, the [*Z*]/[*E*] ratio is about 50:50.[2]

A matter of controversy stems from the acid−base behavior. Hydroxamic acids can be considered as acid species where the dissociation of the more acidic proton ($pK_{AH_2^+}$ = −1.8 to −2.9)[9a] can only be observed in solutions of strong mineral acids; UV measurements indicate that, under such conditions, the O-protonated form prevails over the N-protonated form,[9] even though the N basicity increases with temperature.[9c,10] Concerning the less acidic proton ($pK_{AH}$ = 8−9),[2,3,11,12] the ionization site (NH or OH) is controversial. On the basis of the IR and UV data associated with the acidity measurements, Exner and Kakác[13] suggested that hydroxamic acids are N acids; subsequent works on $^{17}O$ NMR,[7,10,14] FT-IR experiments,[15] N versus O alkylation,[1,16] and recent theoretical calculations also suggest N deprotonation.[3,6,9]

By contrast, Monzyk and Crumbliss[12a] concluded that, in 2 M $NaNO_3$, aceto- and benzohydroxamic (BHA) acids behave as O acids, a suggestion also supported by Ventura et al.[12b] For acetohydroxamic acid (AHA), Bagno et al.[10,17] proposed O deprotonation in water, in agreement with a kinetic study on $Ni^{2+}$/AHA complexation, whose authors assumed that the O anion should prevail in aqueous solutions.[18] However, recent investigations indicate that the two paths can be present simultaneously, with the preference for one or the other depending on the nature of the solvent or the type of substituent.[17] On the other hand, our earlier study on AHA points to the N anion as the favored species in water,[3] but subsequent NMR spectra at pH = 11.5 have shown that both the N and O anions of the *Z* isomer are present in similar concentrations. Concerning BHA, potentiometric results compatible with O and N deprotonation have been reported.[17] Studies on N- and O-methyl derivatives led to the prediction of the experimental $pK_{AH}$ values of BHA as a combination of the $pK_{AH}$ values of the methylated forms; however, some observed irregularities were attributed to solvent effects.[10,12a,16c,19a] Taking as a reference the reaction of isopropyl methylphosphonofluoridate with BHA and its O- and N-methyl derivatives, Steinberg and Swidler also concluded that, in aqueous solutions, $O^-$ and $N^-$ benzohydroxamate are present in similar concentrations.[19b]

To gain some additional insight into the chemistry of nonsubstituted hydroxamic acids, BHA has been investigated by ab initio calculations in the gas phase, acetone and water, NMR in acetone, and kinetic measurements in water. The theoretical interatomic distances were combined successfully to interpret the nuclear Overhauser enhancement spectroscopy (NOESY) spectra and the subsequent assignment of the NMR signals of the *Z* and *E* protons, whose acid−base properties have been investigated for the first time. Moreover, the kinetic behavior of the BHA/$Ni^{2+}$ complexation reaction can help to provide useful information on the reactive forms of BHA and its anion in water. NMR spectra are not feasible in water because of the low solubility of BHA and also because the OH and NH protons could not be distinguished as a result of their very fast exchange rates.

## Results and Discussion

**Theoretical Calculations.** BHA is, in principle, susceptible to all four conformations shown in Scheme 1. When the amide−imide isomerism and the C−N and O−H internal rotations are considered, BHA presents nonrigid properties and a total of nine minima in the potential energy surface.

(5) (a) Brown, D. A.; Glass, W. K.; Mageswaran, R.; Mohammed, S. A. *Magn. Reson. Chem.* **1991**, *29*, 40−45. (b) Brown, D. A.; Cuffe, L. P.; Fitzpatrick, G. M.; Fitzpatrick, N. J.; Glass, W. K.; Herlihy, K. M. *Collect. Czech. Chem. Commun.* **2001**, *66*, 99−108.
(6) (a)Yamin, J. L.; Ponce, C. A.; Estrada, M. R.; Vert, F. T. *THEOCHEM* **1996**, *360*, 109−117. (b) El Yazal, J.; Pang, Y. P. *J. Phys. Chem. A* **1999**, *103*, 8346−8350. (c) Decouzon, M.; Exner, O.; Gal, J. F.; Maria, P. C. *J. Org. Chem.* **1990**, *55*, 3980−3981.
(7) Lipczynska-Kochany, E.; Iwamura, H. *J. Org. Chem.* **1982**, *47*, 5277−5282.
(8) Brown, D. A.; Coogan, R. A.; Fitzpatrick, N. J.; Glass, W. K.; Abukshima, D. A.; Shiels, L.; Ahlgrén, M.; Smolander, K.; Pakkanen, T. T.; Peräkylä, M. *J. Chem. Soc., Perkin Trans. 2* **1996**, 2673−2679.
(9) (a) Garcia, B.; Ibeas, S.; Hoyuelos, F. J.; Leal, J. M.; Secco, F.; Venturini, M. *J. Org. Chem.* **2001**, *66*, 7896−7993. (b) Muñoz-Caro, C.; Senent, M. L.; Ibeas, S.; Leal, J. M. *J. Org. Chem.* **2000**, *65*, 405−410. (c) Ibeas, S.; García, B.; Leal, J. M.; Senent, M. L.; Niño, A.; Muñoz-Caro, C. *Chem.−Eur. J.* **2000**, *6*, 2644−2652.
(10) Bagno, A.; Comuzzi, C.; Scorrano, G. *J. Am. Chem. Soc.* **1994**, *116*, 916−924.
(11) *Tables of Rates and Equilibrium Constants of Heterocyclic Organic Reactions*; Palm, V. A., Ed.; VINITI: Moscow, 1975.
(12) (a) Monzyk, B.; Crumbliss, A. L. *J. Org. Chem.* **1980**, *45*, 4670−4675. (b) Ventura, O. N.; Rama, J. B.; Turi, L.; Dannerberg, J. J. *J. Am. Chem. Soc.* **1993**, *15*, 5754−5761.
(13) Exner, O.; Kakác, B. *Collect. Czech. Chem. Commun.* **1963**, *28*, 1656−1663.
(14) Exner, O.; Holubek, J. *Collect. Czech. Chem. Commun.* **1965**, *30*, 940−951.
(15) Taylor, R. J.; May, I.; Wallwork, A. L.; Denniss, I. S.; Hill, N. J.; Galkin, B. Y.; Zilberman, B. Y.; Fedorov, Y. S. *J. Alloys Compd.* **1998**, *271*, 534−537.
(16) (a) Bordwell, F. G.; Fried, H. E.; Hughes, D. L.; Lynch, T. S.; Satish, A. V.; Whang, Y. E. *J. Org. Chem.* **1990**, *55*, 3330−3336. (b) Bordwell, F. G.; Liu, W. Z. *J. Am. Chem. Soc.* **1996**, *118*, 8777−8791.
(17) (a) Bagno, A.; Scorrano, G. *J. Phys. Chem.* **1996**, *100*, 1536−1544. (b) Bagno, A.; Dorigo, F.; McCrae, P.; Scorrano, G. *J. Chem. Soc., Perkin Trans. 2* **1996**, 2163−2168.
(18) Dominey, L. A.; Kustin, K. *Inorg. Chem.* **1984**, *23*, 103−108.
(19) (a) Exner, O.; Hradil, M.; Mollin, J. *Collect. Czech. Chem. Commun.* **1993**, *58*, 1109−1121. (b) Swidler, R.; Steinberg, G. M. *J. Am. Chem. Soc.* **1956**, *78*, 3594−3958.

**Table 1.** Relative Energies (kcal mol$^{-1}$) and Dipole Moments ($\mu$) of the Neutral BHA and Anions Forms in the Gas Phase

| | RHF/cc-pVDZ | | B3LYP/AUG-cc-pVDZ | |
|---|---|---|---|---|
| | $E_R$ | $\mu$ | $E_R$ | $\mu$ |
| | | Neutral Forms | | |
| *Z* amide | 0.0[a] | 3.8430 | 0.0[c] | 3.7444 |
| *E* amide | 3.7 | 3.0209 | 5.8 | 3.0294 |
| *Z* imide | 3.4 | 0.2481 | 2.5 | 0.3787 |
| *E* imide | 10.1 | 0.2759 | 8.7 | 0.4013 |
| | | Anions | | |
| *Z* anion Ia | 0.0[b] | 8.6088 | 0.0[d] | 8.1563 |
| *Z* anion Ib | 20.0 | 9.5964 | 12.2 | 6.5022 |
| *Z* anion II | 25.6 | 13.2249 | 14.1 | 11.1306 |
| *E* anion Ia | 16.3 | 7.3017 | 16.5 | 6.9976 |
| *E* anion Ib | 29.9 | 7.4107 | 21.8 | 6.8407 |
| *E* anion II | 13.8 | 7.2299 | 9.6 | 6.5150 |

[a] $E_a = -473.323\,413$ au. [b] $E_b = -472.746\,235$ au. [c] $E_c = -476.184\,605$ au. [d] $E_d = -472.636\,498$ au.

**Table 2.** Dissociation Energies (kcal mol$^{-1}$) of BHA Calculated with (a) RHF/cc-pVDZ (gas phase), (b) B3LYP/AUG-cc-pVDZ (gas phase), (c) B3LYP/AUG-cc-pVDZ +PCM (water), and (d) B3LYP/AUG-cc-pVDZ + PCM (acetone)

| RHF/cc-pVDZ (gas phase) | | | |
|---|---|---|---|
| *Z* amide ⇌ *Z* anion Ia | 362.2 | *E* amide ⇌ *E* anion Ia | 374.8 |
| *Z* amide ⇌ *Z* anion II | 387.8 | *E* amide ⇌ *E* anion II | 372.3 |
| *Z* imide ⇌ Z anion Ib | 378.8 | *E* imide ⇌ *E* anion Ib | 382.0 |
| B3LYP/AUG-cc-pVDZ (gas phase) | | | |
| *Z* amide ⇌ *Z* anion Ia | 343.9 | *E* amide ⇌ *E* anion Ia | 354.6 |
| *Z* amide ⇌ *Z* anion II | 358.0 | *E* amide ⇌ *E* anion II | 347.7 |
| *Z* imide ⇌ *Z* anion Ib | 351.1 | *E* imide ⇌ *E* anion Ib | 356.9 |
| B3LYP/AUG-cc-pVDZ+PCM (water) | | | |
| *Z* amide ⇌ *Z* anion Ia | 299.4 | *E* amide ⇌ *E* anion Ia | 307.3 |
| *Z* amide ⇌ *Z* anion II | 303.4 | *E* amide ⇌ *E* anion II | 302.1 |
| B3LYP/AUG-cc-pVDZ+PCM (acetone) | | | |
| *Z* amide ⇌ *Z* anion Ia | 301.0 | *E* amide ⇌ *E* anion Ia | 309.2 |
| *Z* amide ⇌ *Z* anion II | 305.8 | *E* amide ⇌ *E* anion II | 303.8 |

This work pursues characterizing all of the possible deprotonation processes, and a detailed search of all stable conformations from different starting points has been performed. A full characterization of these structures, which implies a rather large computational effort, has not been performed previously at this level of refinement. Furthermore, if the acid dissociation process is also considered, then an accurate determination of the relative energies of the anionic forms requires the use of basis sets containing diffuse orbitals (AUG-cc-pVDZ). The computational expenses have been minimized using the density functional theory instead of the perturbation theory. Initially, the calculations were performed at the RHF/cc-pVDZ level, which is a tool powerful enough for the search of minimum energy structures, by optimizing the geometry from distinct starting configurations. Hence, starting from the most stable RHF structures, more accurate B3LYP/AUG-cc-pVDZ calculations with full geometry optimization have been performed in order to determine the relative energies and the enthalpies of the most probable deprotonation processes. The B3LYP/AUG-cc-pVDZ approximation reduces the dissociation energy values calculated with RHF/cc-pVDZ.

**Scheme 2.** Theoretical Deprotonation Processes of *Z* and *E* BHA

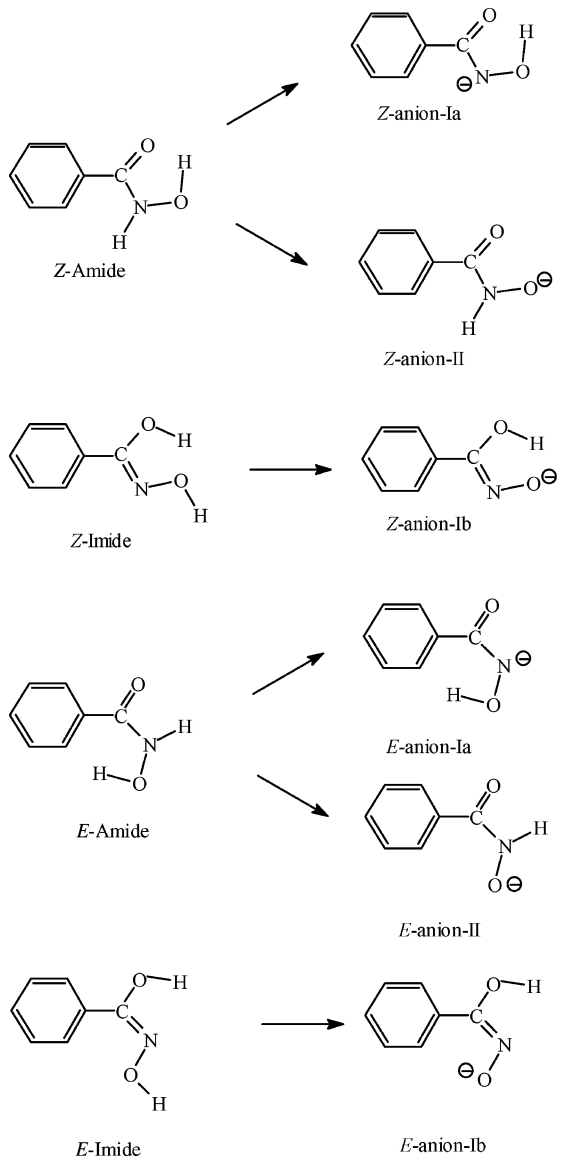


The BHA forms, where the aromatic ring and the N−C═O group are coplanar, have been taken as starting structures for geometry optimization. The imide forms and the anions are planar, whereas the nitrogen of the amide forms adopts the pyramidal structure. Table 1 summarizes the RHF/cc-VDZ relative energies and dipole moments of the neutral forms and anions of BHA.

An accurate determination of the energies requires the use of large basis sets.[10] Our calculations point to *Z* amide as the most stable neutral BHA form in the gas phase. The probabilities of the existence of the *E*-amide, *Z*-imide, and *E*-imide isomers are much lower than that of the *Z* amide. Actually, assuming that the relative energy values could represent free energy changes, the data of Table 1 yield the population ratios in the gas phase, [*E* amide]/[*Z* amide] = $1.4 \times 10^{-3}$ and [*Z* imide]/[*Z* amide] = $3.2 \times 10^{-3}$ at 298 K. Imide-like structures of hydroxamic acids have a low probability of existence in aqueous solutions as well; although these structures were postulated to form during the syntheses of hydroxamic acids from amide and hydro-

**Table 3.** Distances ($10^{-8}$ cm) between the Dissociable Protons and the Aromatic Ortho-Hydrogen Atoms Calculated with the B3LYP/AUG-cc-pVDZ Method for the *Z*-Amide and *E*-Amide Forms of BHA

| *Z*-amide | | | | *E*-amide | | | |
|---|---|---|---|---|---|---|---|
| | isolated molecule | +water | +acetone | | isolated molecule | +water | +acetone |
| H(2)−(O)H$_Z$ | 4.4072 | 4.4309 | 4.4302 | H(2)−(O)H$_E$ | 2.9791 | 3.0212 | 3.0072 |
| H(2)−(N)H$_Z$ | 2.4044 | 2.2892 | 2.3114 | H(2)−(N)H$_E$ | 3.7009 | 3.8212 | 3.8163 |
| H(6)−(O)H$_Z$ | 4.4081 | 4.4196 | 4.4144 | H(6)−(O)H$_E$ | 4.5181 | 4.5204 | 4.5070 |
| H(6)−(N)H$_Z$ | 4.2841 | 4.4488 | 4.4374 | H(6)−(N)H$_E$ | 4.4700 | 4.4673 | 4.4659 |

xylamine,[20] they are actually only unstable reaction intermediates that may evolve to the corresponding C═O compounds, because protonation of the carbonyl residue is difficult and can be achieved only in concentrated strong acid solutions.[9a]

Ab initio calculations on AHA, performed with the same method, show that the *Z*-amide isomer is prevailing for this compound also;[3] however, the probability of the *Z*-imide form is much higher than that for BHA, the ratio being [*Z* imide]/[*Z* amide] = 0.156 at 298 K. This feature could be due to the replacement of the $C_6H_5-$ group by the $CH_3-$ group with opposite electronic properties. The enhanced stability of the *Z*-amide form can be due to the formation of an intramolecular hydrogen bridge between the oxygen atoms in the cis position. By contrast, the isolated molecules of the *Z*-imide or *E*-amide configurations are prevented from this possibility. It should be noted that recent calculations on AHA[3,6b] yielded a difference between the *E* and *Z* isomers less than the hydrogen bond energy (2−5 kcal mol$^{-1}$);[21] on this basis, the authors concluded that the intramolecular H bond is disabled in the *Z* form.[6b] This is not the case for BHA, because the calculated energy difference of 5.8 kcal mol$^{-1}$ between *E* and *Z* (Table 1) is a value well-above the chemical accuracy (ca. 2 kcal mol$^{-1}$).[20]

The deprotonation of BHA can produce six different anions according to the dissociation paths shown in Scheme 2. Although a general equilibrium Scheme can, in principle, be established between all of the acid forms and between all of the anions, and from the equilibrium mixture of the acids one could get the equilibrium mixture of the anions, Table 1 shows that *Z* anion Ia is by far the most stable and the $Z \rightleftharpoons E$ interconversion is hindered by relatively high barriers, as already observed.[3,5,6,9] Therefore, it has been assumed that, in the gas phase, the deprotonation processes of the *Z* forms produce *Z* anions, whereas those of the *E* forms produce *E* anions. This assumption enables the two types of processes to be studied independently. The deprotonation energies of the conformers shown in Scheme 2 are collected in Table 2. The two levels of calculation would indicate that, in the gas-phase, N deprotonation of the *Z*-amide form is favored by far with respect to O deprotonation.

The dissociation energies of *Z* amide and *E* amide have been calculated in the presence of water and acetone (Table 2). The solvent effect has been considered by means of the polarizable continuum model (PCM) method,[22,23] in which the solvent is regarded as a continuum dielectric, characterized by a constant permittivity. The N deprotonation of the *Z* amide and the O deprotonation of the *E* amide are the most probable processes in all three of the investigated systems, and the relative energies, which depend on the solvation energies of the anionic species, decrease when the dielectric constant of the solvent is raised.

The distances between all BHA atoms, calculated with B3LYP/AUG-cc-pVDZ, are given in the Supporting Information, whereas the distances between the acidic H atoms and the aromatic ortho-H [H(2) and H(6)] atoms of both the *Z*-amide and *E*-amide forms are listed in Table 3 and will be employed to interpret the NMR results.

**$^1$H NMR Spectroscopy.** The NMR measurements were performed in acetone. Figure 1 shows a $^1$H NMR spectrum of BHA recorded at −80 °C. The solvent signal falls at 2.09 ppm, outside the plot. The signal at 3.66 ppm corresponds to the residual trace $H_2O$, as the addition of external water to the acetone solution confirms; the set of signals at around 7.7 ppm correspond to the protons of the aromatic ring. The electron withdrawing from the ring by the hydroxamate group (- M effect) indicates that the protons more affected by the mesomeric substituent effect are the ortho-H protons, with $\delta = 7.85$ ppm, followed by the para-H protons, with $\delta = 7.58$ ppm, and the meta-H protons, with $\delta = 7.49$ ppm. The remaining four signals, 1 (11.46 ppm), 2 (11.06 ppm), 3 (10.01 ppm), and 4 (6.54 ppm), should be assigned to the protons of different configurations of the amide form of BHA; such configurations must correspond to the *Z* and *E* isomers of the hydroxamate group (in Scheme 1, *Z* amide and *E* amide, respectively) because the formation of the imide forms in solution was found to be negligible.[10,16c,18,19] The measured area ratios area 1/area 2 = area 3/area 4 = 75:25 indicate that signals 1 and 3 correspond to one isomer, which represents 75%, and signals 2 and 4

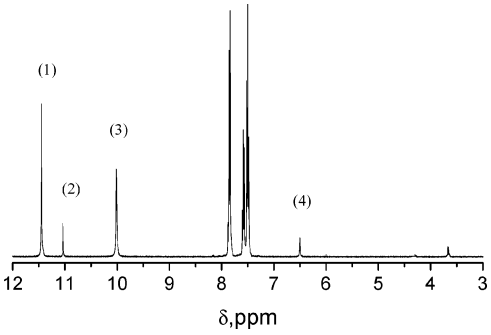


**Figure 1.** $^1$H NMR spectra of BHA in acetone-$d_6$. $T = -80$ °C; $C_{BHA} = 0.032$ M.

(20) Jencks, W. P.; Gilchrist, M. *J. Am. Chem. Soc*. **1964**, *86*, 5616−5620.
(21) (a) Jeffrey, G. A.; Saenger, W. *Hydrogen Bonding in Biological Structures*; Springer-Verlag: Berlin, Germany, 1991. (b) Scheiner, S. *Hydrogen Bonding. A Theoretical Perspective*; Oxford University Press: New York, 1997.
(22) Tomasi, J.; Persico, M. *Chem. Rev*. **1994**, *94*, 2027−2094.
(23) Barone, M.; Cossi, B.; Mennucci, B.; Tomasi, J. *J. Chem. Phys*. **1997**, *107*, 3210−3221.

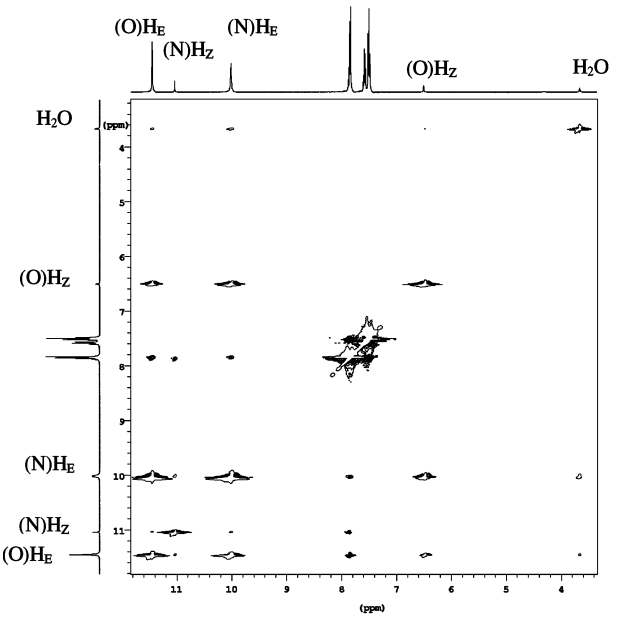


**Figure 2.** $^1$H−$^1$H NMR 2D NOESY spectra of BHA in acetone-$d_6$. $T = -80$ °C; $C_{BHA} = 0.032$ M.

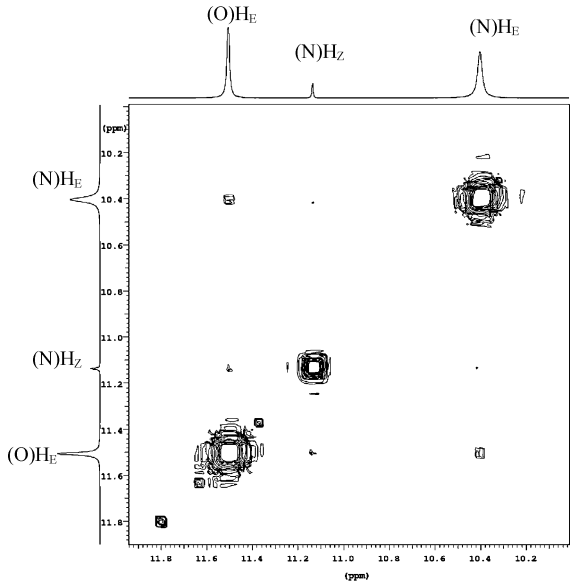


**Figure 3.** $^1$H−$^1$H NMR 2D COSY spectra of BHA in acetone-$d_6$. $T = -60$ °C; $C_{BHA} = 0.032$ M.

correspond to the other, which represents 25% of the total BHA population in acetone.

**Signal Assignment.** Figure 2 shows the 2D NOESY spectra of BHA at −80 °C. Some crosspeaks due to chemical exchange (empty dots) and spin decoupling contacts (black dots) were observed. A spin decoupling effect was observed between the aromatic ortho H and the signals labeled as 1, 3 (majority isomer), and 2 (minority isomer) in Figure 1. These results reveal that the two protons of the majority isomer (signals 1 and 3) and only one of the two protons of the minority isomer (signal 2) fulfill the requirement of vicinity to the aromatic ortho H. It should be noted that, in NOESY spectra, spin decoupling could only be observed between $^1$H nuclei and over a distance of about 4 Å.[24a] Table 3 shows that all three, (O)H$_E$, (N)H$_E$, and (N)H$_Z$, fulfill this condition in the isolated molecule, in water, and in acetone. Therefore, signals 1 (11.46 ppm) and 3 (10.01 ppm) must correspond to the *E* isomer, which, in turn, is the major species in acetone. Signal 2 (11.06 ppm) is ascribed to the (N)H$_Z$ proton, whereas signal 4 (6.50 ppm), which does not exhibit spin decoupling, is assigned to the (O)H$_Z$ proton because its distance from both H(2) and H(6) exceeds 4 Å. A comparison of the data of Table 3 with the intensities of signals 1 and 3 enables one to deduce which of them should be ascribed to the (O)H$_E$ and which should be ascribed to the (N)H$_E$ forms. The H(2)−(O)H$_E$ distance is smaller than the H(2)−(N)H$_E$ distance, and , therefore, more intense interaction results in the first case. Figure 2 shows that the most intense of the three black dots corresponds to signal 1 (11.46 ppm), which should then be assigned to the (O)H$_E$ proton. Subsequently, signal 3 (10.013 ppm) is assigned to the (N)H$_E$ proton. These results were confirmed by a 1D NOESY spectra (not shown) performed at −80 °C; irradiation of the sample at the resonance frequencies of (O)H$_E$ ($\delta = 11.46$ ppm) and (N)H$_E$ ($\delta = 10.01$ ppm) shows that the spin decoupling effect (positive signal) is more intense in the first case.

Further insight into the problem of signal assignment can be gained by 2D $^1$H−$^1$H correlation spectroscopy (COSY) spectra, which enable the assignment of the proton−proton coupling. Spectra recorded at −60 °C (Figure 3) give rise to off-diagonal crosspeaks; two of them, corresponding to the most intense singlets, appear in the figure as points of coordinates (11.51 and 10.40) at both sides of the diagonal. From the matrix coordinates (Supporting Information), the distances between the OH and NH protons of the *Z* and *E* forms were determined as $r_{H,Z} = 2.6529$ Å and $r_{H,E} = 2.4064$ Å, respectively. The two protons of the *E* form are closer together than those of the *Z* form; hence, the observed peaks were assigned to the *E* conformation, consistently with NOESY spectra. Also, the COSY spectra showed weak coupling between the signals of *E* and *Z*, which appear as two points of coordinates, 11.14 and 11.51 ppm, at both sides of the diagonal; we will come to this point below.

In conclusion, a full assignment of the BHA singlets (shown in the axes of Figure 2 and partly in Figure 3) in increasing order of $\delta$, (O)H$_Z$ < (N)H$_E$ < (N)H$_Z$ < (O)H$_E$, is feasible by combining NMR spectra at low temperatures with the interatomic distances obtained by ab initio calculations; NMR spectra reveal that, in acetone, BHA is present mainly as the *E* conformation, the *Z* conformation being only 25% of the total population. This conclusion should be emphasized because, formerly, it was believed that the BHA *Z* isomer is the only one present both in solution[7,8,10] and in the solid state.[7,25] It should be pointed out, however, that experiments on N-phenyl-BHA have shown that the [*Z*]/[*E*] ratio strongly

(24) Silverstein, R. M.; Webster, F. X. *Spectrometric Identification of Organic Compounds*, 6th ed.; John Wiley & Sons: New York, 1998; (a) p 189; (b) p 166.

(25) Smith, W. L.; Raymond, K. N. *J. Am. Chem. Soc.* **1980**, *102*, 1252−1255.

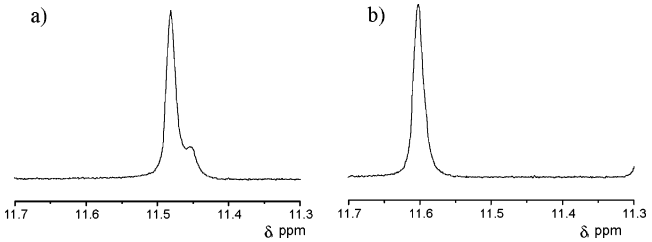


**Figure 4.** $^1$H NMR spectra of BHA in acetone covering the region of the (O)$H_E$ resonance. The content of the $H_2O$ traces of experiment b is 46 times that of experiment a. $T = -80$ °C; $C_{BHA} = 0.032$ M.

depends on the nature of the solvent.[2] Acetone is a dipolar aprotic, not an H-bond donor, with a large relative permittivity ($\epsilon_r = 20.56$), sizable dipole moment ($\mu = 2.7$ D), and solvent polarity ($E_T^N = 0.355$),[26] and is capable of stabilizing the *E* form with respect to the less-polar *Z* form.

**Chemical Exchange.** The set of off-diagonal empty dots in Figure 2 reveals the occurrence of chemical exchange among the different configurations and with residual $H_2O$ (note that traces of water are present in acetone). It should be noted that, at −80 °C, both the (O)$H_E$ and (N)$H_E$ protons exchange with $H_2O$ but (O)$H_Z$ and (N)$H_Z$ do not. This finding can be interpreted, assuming that the protons of the *Z* configuration are blocked by H bonding. An increase in the temperature or in the water content reduces the intramolecular strength of the H bonds, and as a consequence, the protons of the *Z* form can also exchange with $H_2O$. This is shown in Figure 1 of the Supporting Information, which reports 2D NOESY spectra recorded at −60 °C with a water content 1.3 times that of the experiment of Figure 2.

**Dimer Formation in Acetone.** Figure 4 shows two $^1$H NMR spectra recorded in acetone at −80 °C in the region corresponding to the (O)$H_E$ resonance. The spectra differ by the content of $H_2O$ traces, which, in experiment 4b, is 46 times that of experiment 4a. Changing the water content causes chemical shifts; for instance, the (O)$H_E$ signal moves as shown in Figure 4: (N)$H_Z$ moves from 11.08 ppm (a) to 11.30 ppm (b), (N)$H_E$ moves from 10.11 ppm (a) to 10.03 ppm (b), (O)$H_Z$ moves from 6.57 ppm (a) to 6.68 ppm (b), and the water signal moves from 3.70 ppm (a) to 4.08 ppm (b). All of the signals move to lower fields except that of (N)$H_E$; this feature is ascribable to the lower H-bond strength of (N)$H_E$ the higher the water content and points to the formation of stable *E*−*E* dimers in acetone. Spectrum a shows two different signals in a 2:1 area ratio; spectrum b, though apparently displaying a single signal, in fact is composed of two Gaussians whose deconvolution yields a 50:1 area ratio.

These findings indicate the presence of two forms of the *E* isomer whose amounts depend on the water content. This behavior could be rationalized, assuming that the *E* isomer is distributed between a monomer and a dimer in an equilibrium that shifts toward the monomer as the water content increases. Similarly, the spectral deconvolution of the signals corresponding to the (N)$H_Z$ resonance show that these signals are also composed of two Gaussians. Although the signal-to-noise ratio is, in this case, too low to enable an evaluation of the area ratio, the composite nature of the signal can be interpreted assuming a monomer ⇌ dimer equilibrium for the *Z* isomer as well.

**Table 4.** Effect of the BHA Concentration on Chemical Shifts in Acetone, $T = -80$ °C

| $C_{BHA}$ M | $\delta$ O(H)$_E$ ppm | $\delta$ N(H)$_Z$ ppm | $\delta$ N(H)$_E$ ppm | $\delta$ O(H)$_Z$ ppm |
|---|---|---|---|---|
| 0.022 | 11.448 | 11.055 | 9.928 | 6.487 |
| 0.032 | 11.458 | 11.061 | 10.013 | 6.504 |
| 0.035 | 11.467 | 11.065 | 10.034 | 6.530 |
| 0.048 | 11.481 | 11.073 | 10.147 | 6.571 |

**Scheme 3.** Dimers *E*−*E* (A), *Z*−*Z* (B), and Aggregates *E*−*Z* (C)

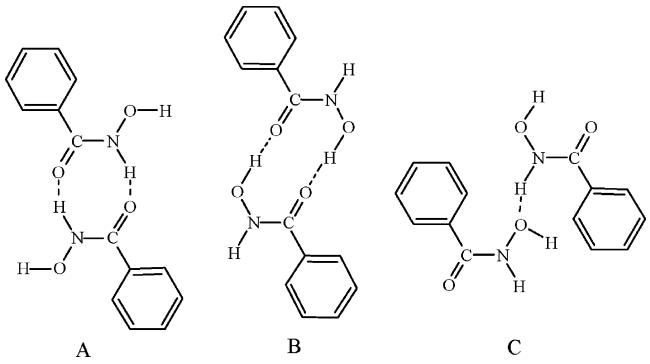


The formation of *E*−*E* and *Z*−*Z* dimers is also supported by the effect of BHA concentration on the chemical shifts, as shown by the data at −80 °C (Table 4). The significant variation of the chemical shift for (N)$H_E$ and the splitting of the (O)$H_E$ singlet (Figure 4) may be ascribable to the existence of stable *E*−*E* intermolecular H bonds (Scheme 3), similar to those reported for dimers of carboxylic acids and amides[24b,26] and nonsubstituted hydroxamic acids.[8] On the other hand, the concentration effect on the (O)$H_Z$ signal points to the formation of *Z*−*Z* dimers as well (Scheme 3), as observed for N-phenyl-BHA in acetone.[2] Further, COSY spectra (Figure 3) show crosspeaks between (O)$H_E$ and (N)$H_Z$ (weak dots of coordinates 11.14 and 11.51 outside the diagonal), indicating the possible formation of aggregates by (N)$H_Z$−(O)$H_E$ hydrogen bridges, a suggestion justified by the weak coupling between the protons of the two isomers. These results justify the configurations depicted in Scheme 3.

**Dynamic NMR.** Figure 5 shows the $^1$H NMR spectra recorded between −80° and 40 °C; the aromatic proton signals are not included for simplicity. The spectra deduced by line shape simulations, superimposed to the experimental ones, are based on a model that includes *E*−*E*, *Z*−*Z*, and *E*−*Z* proton exchanges; the exclusion of one of the three processes introduces remarkable deviations from the experiments. Interexchange with water was excluded because the spectra of Figure 5 were performed after careful drying of both the solute and solvent to reduce trace water to a minimum; the simulated and experimental spectra are in full agreement. Table 5 lists the rate constants for hydrogen intraexchange ($k_{EE}$ and $k_{ZZ}$) and interexchange ($k_{EZ}$) evaluated

(26) Reichardt, C. *Solvents and Solvent Effects in Organic Chemistry*, 3rd ed.; Wiley-VCH: New York, 2003.

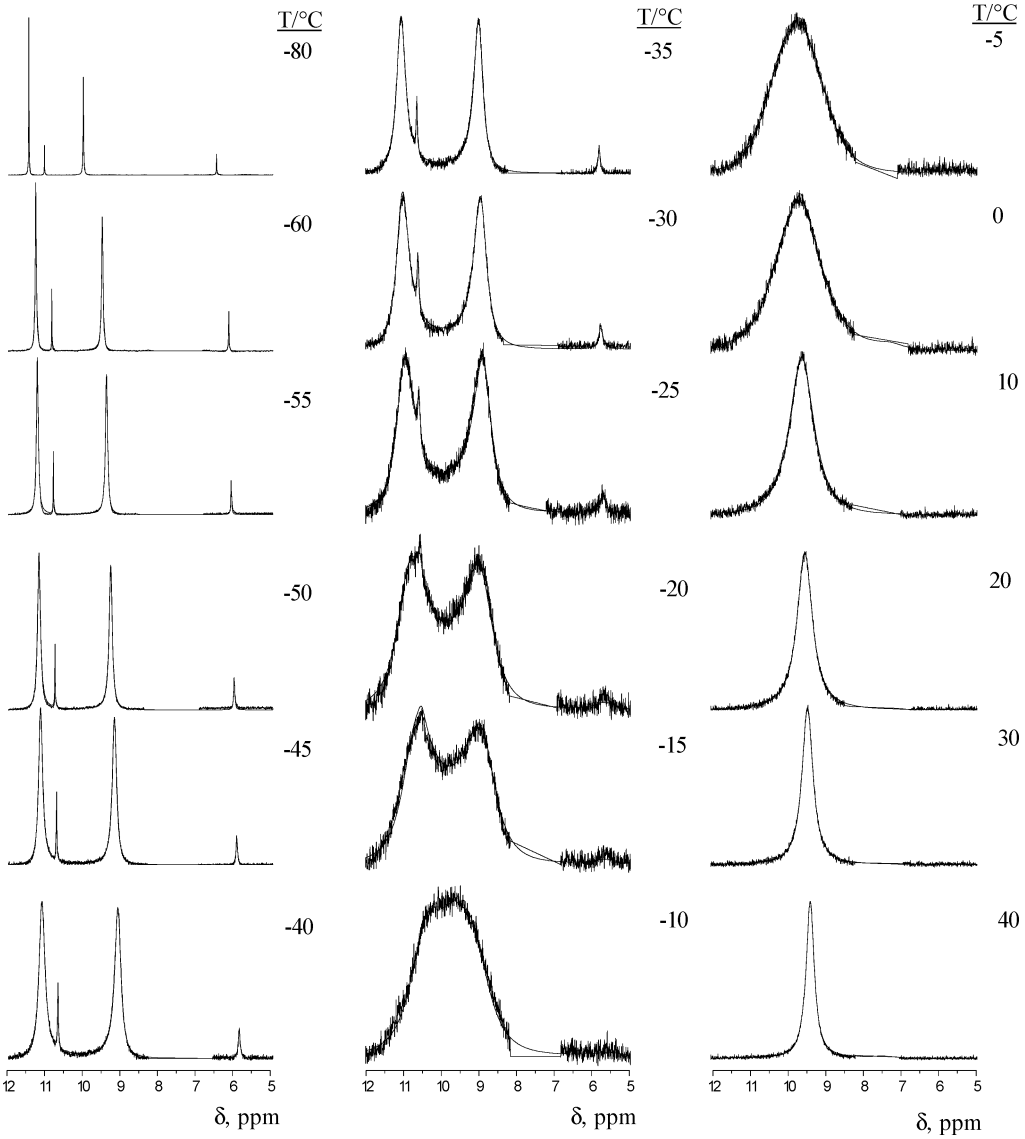


**Figure 5.** $^1$H NMR spectra of BHA in acetone-$d_6$ between −80 and +40 °C. The spectra superimposed have been calculated by a line shape simulation. $C_{BHA}$= 0.032 M.

at different temperatures. The ln $k$ versus $1/T$ plot ($R^2 > 0.995$) yields the activation parameters summarized in Table 6.

The coalescence between the singlets of the protons of the *E* isomer occurring at −10 °C indicates a fast exchange between them. Increasing the residual $H_2O$ by 30% causes the coalescence to occur at 5 °C (Figure 2 in the Supporting Information); this feature indicates that water hinders the interchange between the two protons of the −NHOH group, probably because of H-bond formation with water, as shown in Scheme 4.

The chemical exchange data show that the presence of the two isomers can be detected below room temperature; hence, it is not surprising that previous contributions at room temperature could only report one isomer in BHA.[7,8,10,19]

Table 5 shows that the rate of proton exchange between $(O)H_E$ and $(N)H_E$ ($k_{EE}$) is high, in accordance with both the evolution of the spectra with temperature (Figure 5) and the strong NOESY effect observed at −80 °C (Figure 2). By contrast, the rate of proton exchange between $(O)H_Z$ and $(N)H_Z$ ($k_{ZZ}$) is low, in accordance with both the slow coalescence of the *Z* singlets (Figure 5) and the absence of crosspeaks between the corresponding singlets (Figure 2). This behavior is consistent with the existence of *intra* H bonding in the BHA *Z* form; when the hydrogen bond is strong, the rate of proton transfer decreases.[27] Such an explanation has already been given for other monosubstituted hydroxamic acids.[5b,7] The rate constant $k_{EZ}$ is higher than $k_{ZZ}$ at low temperatures, and it is lower at high temperatures. The evolution of the singlets in Figure 5 cannot be clearly observed because the $(O)H_E$ and $(N)H_Z$ signals overlap above −20 °C. However, the widening of the signals below −20 °C shows that the exchange between *Z* and *E* is much slower than that between $(O)H_E$ and $(N)H_E$, in accordance with the simulation results.

(27) (a) Eigen, M. *Angew. Chem., Int. Ed. Engl.* **1964**, *3*, 1−19. (b) Eigen, M.; Kruse, W.; Maass, G.; de Maeyer, L. *Prog. React. Kinet.* **1964**, *2*, 285−318. (c) Eigen, M.; Kruse, W. *Z. Naturforsch. B* **1963**, *18*, 857−865.

**Table 5.** Rate Constant Values in Acetone at Different Temperatures for the Hydrogen Intraexchange ($k_{EE}$ and $k_{ZZ}$) and Interexchange ($k_{EZ}$) Processes

| | rate constants, $s^{-1}$ | | |
|---|---|---|---|
| $T$/°C | $k_{EE}$ | $k_{ZZ}$ | $k_{EZ}$ |
| −60 | 28.1 | | 0.167 |
| −55 | 49.8 | | 0.256 |
| −50 | 82 | | 0.351 |
| −45 | 110 | | 0.522 |
| −40 | 172 | | 0.812 |
| −35 | 265 | 0.25 | 1.15 |
| −30 | 370 | 0.451 | 1.58 |
| −25 | 547 | 0.62 | 2.41 |
| −20 | 750 | 1.35 | 3.01 |
| −15 | 1090 | 2.31 | 4.15 |
| −10 | 1450 | 4.1 | 5.23 |
| −5 | 2049 | 6.94 | 7.62 |
| 0 | 2780 | 12.2 | 10.2 |
| 10 | 4800 | 31.2 | 17.3 |
| 20 | 8300 | 80.5 | 27.8 |
| 30 | 13620 | 182 | 43.2 |
| 40 | 26313 | 420 | 69.1 |

**Table 6.** Activation Parameters for the Hydrogen Intraexchange ($k_{EE}$ and $k_{ZZ}$) and Interexchange ($k_{EZ}$) Processes in Acetone

| | $\Delta H^{\ddagger}$/kcal mol$^{-1}$ | $\Delta S^{\ddagger}$/cal K$^{-1}$mol$^{-1}$ |
|---|---|---|
| $k_{EE}$ | 8.31 ± 0.07 | −12.2 ± 0.2 |
| $k_{ZZ}$ | 14.3 ± 0.2 | −1.0 ± 0.7 |
| $k_{EZ}$ | 7.51 ± 0.05 | −26.3 ± 0.2 |

**Scheme 4.** Hydrogen Bonding between the *E* Isomer and Water

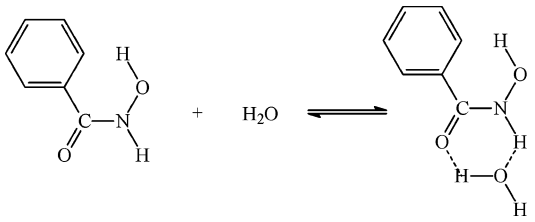

**Table 7.** Acid Dissociaton Constant of BHA (p$K_{HA}$) in Aqueous Solution at Different Temperatures and Thermodynamic Parameters from vant' Hoff Analysis, $I$ = 0.2 M

| $T$/°C | p$K_{HA}$ | $\Delta S$°/cal K$^{-1}$ mol$^{-1}$ | $\Delta H$°/kcal mol$^{-1}$ |
|---|---|---|---|
| 15 | 8.94 ± 0.02 | | |
| 25 | 8.78 ± 0.01 | | |
| | 8.80[19,21] | | |
| | 8.92[25] | | |
| 35 | 8.67 ± 0.01 | | |
| 45 | 8.56 ± 0.03 | | |
| 55 | 8.42 ± 0.02 | | |
| | | −22 ± 0.5 | 5.4 ± 0.2 |

**Relative Acidity of the *E* and *Z* Protons.** To compare the acidities of the BHA protons, two NMR spectra were recorded at −80 °C in the presence of increasing, small amounts of $D_2O$. The behavior of the system is shown in Figure 6. The areas of all of the signals decrease upon increasing the $D_2O$ content, except those of the aromatic protons; the decrease of the signal areas, 75% (peak 1), 73% (peak 3), 89% (peak 2), and 87% (peak 4), indicate that the *Z* isomer is only slightly (12%) more acidic than isomer *E* and also that the acidities of the NH and OH protons within each isomer are similar. The formation of N and O anions in similar concentrations has already been proposed for other hydroxamic acids.[17,19]

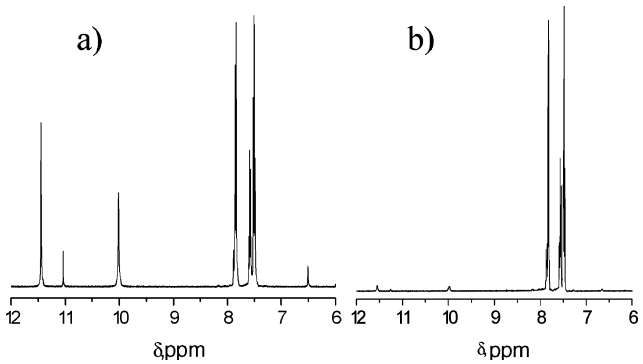


**Figure 6.** NMR spectra of BHA in the presence of $D_2O$. The $D_2O$ content of experiment b is twice that of experiment a. $T$ = −80 °C; $C_{BHA}$ = 0.032 M; solvent = acetone.

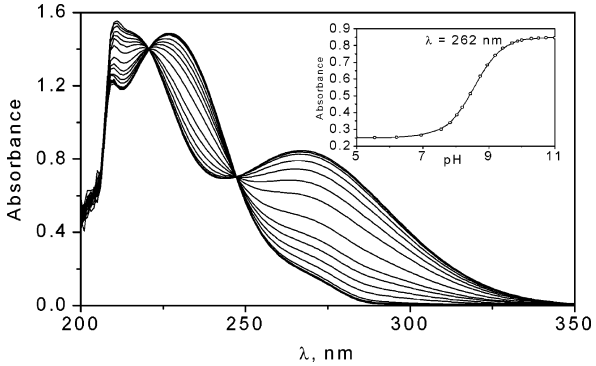


**Figure 7.** Set of spectral curves corresponding to the ionization equilibrium of BHA in aqueous solution. $T$ = 35 °C; $I$ = 0.2 M.

**Dissociation Equilibria.** The acid dissociation process of BHA, reaction 1,

$$HL \rightleftharpoons L^- + H^+ \quad (1)$$

has been investigated by UV spectrophotometry using a procedure described previously.[2,3] Figure 7 shows the set of UV spectra recorded during the titration performed at 35 °C. For comparison, the p$K_{HA}$ value was determined as well by analyzing the change during titration of the visible spectra of thymol blue, added as an indicator to the BHA/NaOH system.[2] The temperature dependence of $K_{HA}$ was investigated at 15, 25, 35, 45, and 55 °C. A van't Hoff analysis ($R^2$ > 0.997) yields the dissociation enthalpy and entropy values. The equilibrium parameters of reaction 1 listed in Table 7 are in agreement with others already published.[12a]

**Complex Formation between Ni(II) and BHA. Equilibria.** The interaction of BHA with Ni(II) is revealed by the change that occurs in the UV spectrum of the acid upon metal addition (Figure 8). Under metal excess conditions ($C_M \gg C_L$), only 1:1 complexes are formed. At a constant pH, the equilibria could be described by the apparent complex formation reaction

$$M_f + L_f \underset{k_d}{\overset{k_f}{\rightleftharpoons}} ML_f \quad (2)$$

where $[M_f] = [M^{2+}]$, $[L_f] = [HL] + [L^-]$, and $[ML_T] = [MHL^{2+}] + [ML^+]$.

The equilibrium constant of reaction 2, $K_{app}$, was obtained from spectrophotometric titrations (280 nm) of BHA with

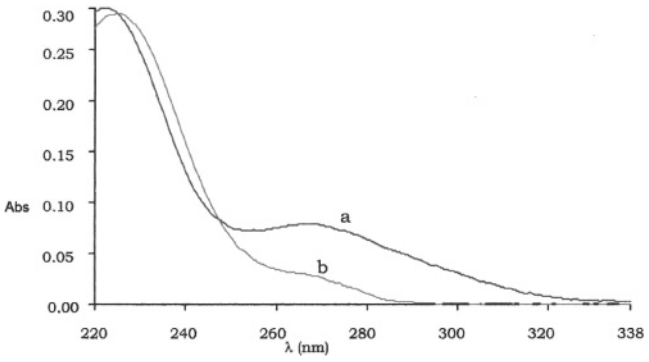


**Figure 8.** Absorption spectra of the BHA/Ni(II) system in aqueous solution at pH 6.5, $I = 0.2$ M, and $T = 25$ °C: (a) $4 \times 10^{-5}$ M BHA; (b) $4 \times 10^{-5}$ M BHA + $5 \times 10^{-3}$ M $Ni(ClO_4)_2$.

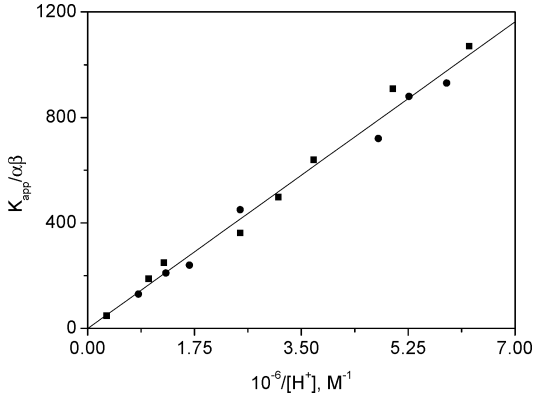


**Figure 9.** Dependence of the apparent equilibrium constant, $K_{app}$, on the reciprocal hydrogen ion concentration for the BHA/Ni(II) system in aqueous solution. $I = 0.2$ M and $T = 25$ °C: (●) kinetic data; (■) thermodynamic data.

$Ni(ClO_4)_2$. The binding curves were analyzed according to a previously described procedure.[28] The $K_{app}$ values were found to depend on $[H^+]$ according to eq 3

$$K_{app}/\alpha\beta = K_{MHL} + K_{ML}K_{HA}/[H^+] \quad (3)$$

which has been derived on the basis of the reactions in Scheme 5.

**Scheme 5**

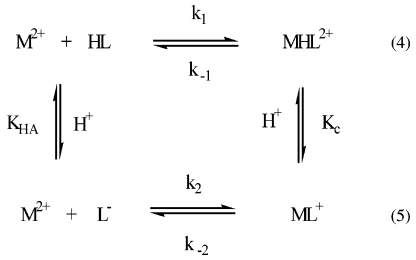


$K_{MHL}(=k_1/k_{-1})$ and $K_{ML}$ $(=k_2/k_{-2})$ are the equilibrium constants of steps 4 and 5, respectively, whereas $\alpha = [HL]/[L_f]$ and $\beta = [M^{2+}]/[M_f]$. Figure 9 shows a plot of $K_{app}/\alpha\beta$ versus $1/[H^+]$. According to eq 3, the slope value divided by $K_{HA}$ provides the value of $K_{ML}$ quoted in Table 8. The intercept is close to zero, indicating that the $K_{MHL}$ value is small and that step 4 yields a negligible contribution to the thermodynamics of the system. Under these circumstances, eq 3 could be rearranged to give

$$K_{ML} = K_{app}K_{HA}^{-1}\alpha^{-1}\beta^{-1}[H^+] \quad (6)$$

Values of $K_{app}$ were obtained at four different temperatures between 293 and 308 K. The van't Hoff analysis yielded the values of $\Delta H_{app}°$ and $\Delta S_{app}°$, which, with the aid of eq 6, provide the thermodynamic parameters of reaction 5 listed in Table 8.

**Kinetics.** The kinetic curves for complex formation are single exponential (Figure 3 in the Supporting Information), indicating that the apparent reaction 2 could adequately represent the kinetic behavior of the BHA/Ni(II) system. It has been found that, for $C_M \gg C_L$, the time constant $1/\tau$ is independent of the BHA concentration but depends on the metal concentration, according to eq 7, as shown in Figure 10.

$$\frac{1}{\tau} = k_d + k_f C_M \quad (7)$$

The apparent rate constants $k_f$ and $k_d$ were found to depend on medium acidity, according to the relationships

$$k_f = (k_1 + k_2K_{HA}/[H^+])\alpha\beta \quad (8)$$

and

$$k_d = (k_{-2} + k_{-1}[H^+]/K_C)\gamma \quad (9)$$

where $\gamma = [ML]/[ML_T] \cong 1$. The $k_f/\alpha\beta$ versus $1/[H^+]$ plot (Figure 11a) enables one to obtain $k_1$ and $k_2$, the forward rate constants of steps 4 and 5, respectively, whereas the $k_d/\gamma$ versus $[H^+]$ plot (Figure 11b) yields $k_{-1}/K_C$ and $k_{-2}$.

The temperature dependence of $K_{app}$, $k_f$, and $k_d$ was investigated at pH = 6.5 and at 15, 25, 35, and 45 °C. The reaction parameters are listed in Table 8.

The process of $Ni^{2+}$ binding to most ligands occurs according to the $I_d$ mechanism, where the diffusion-controlled encounter of the two reaction partners leads to the formation of an outersphere complex that loses a water molecule in a subsequent, rate-determining step.[29] The rate of ligand penetration into the inner solvation shell of the metal ion, $k^*$, is related to the rate of solvent exchange, $k_{H_2O}$, by the equation $k^* = Sk_{H_2O}$ where $S$ is a statistical factor equal to 0.75.[30] For $Ni^{2+}$, $k_{H_2O} = 3.1 \times 10^4$ $s^{-1}$.[31] The equilibrium constant, $K_{OS}$, for the step of formation of the outersphere complex can be calculated by the Fuoss equation[32] with a maximum uncertainty of 300% (mainly because of the arbitrary choice of the distance of closest approach of the reactants). The values of $k^*$ can be calculated as $k^* = k/K_{OS}$. We have chosen $Ni^{2+}$ as the candidate to bind BHA because any deviation from the relationship $k^* = Sk_{H_2O}$ should be ascribed to a particular behavior of the ligand. When, for

(28) Secco, F.; Venturini, M. *J. Chem. Soc., Faraday Trans.* **1993**, *89*, 719−725.
(29) Eigen, M.; Tamm, K. *Z. Elektrochem.* **1962**, *66*, 107−121.
(30) Neely, J. W.; Connick, R. E. *J. Am. Chem. Soc.* **1970**, *92*, 3476−3478.
(31) Burgess, J. *Metal Ions in Solution*; Ellis Horwood Ltd.: Chichester, U.K., 1978.
(32) Fuoss, R. M. *J. Am. Chem. Soc.* **1959**, *80*, 5059−5061.

**Table 8.** Reaction Parameters for the Complex Formation Reaction between Nickel(II) and BHA in Aqueous Solution. $I = 0.2$ M; $T = 25°C$

| $10^{-3}k_1$ ($M^{-1}s^{-1}$) | $10^{-2}k_{-1}$ ($s^{-1}$) | $10^{-5}k_2$ ($M^{-1}s^{-1}$) | $k_{-2}$ ($s^{-1}$) | $10^{-1}K_{MHL}$ ($M^{-1}$) | $10^{-5}K_{ML}$ ($M^{-1}$) | $10^{9}K_{HA}$ (M) |
|---|---|---|---|---|---|---|
| $1.97 \pm 45$ | $1.73 \pm 0.26$ | $1.15 \pm 0.20$ | $1.10 \pm 0.19$ | $1.07 \pm 19$ | $1.39 \pm 0.25$ | $1.20 \pm 0.02$ |
| $10^{5}K_C$ (M) | $\Delta H_f^{\ddagger}$ kcal $mol^{-1}$ | $\Delta S_f^{\ddagger}$ cal $mol^{-1}$ $K^{-1}$ | $\Delta H_d^{\ddagger}$ kcal $mol^{-1}$ | $\Delta S_d^{\ddagger}$ kcal $mol^{-1}$ $K^{-1}$ | $\Delta H°_{app}$ kcal $mol^{-1}$ | $\Delta S°_{app}$ cal $mol^{-1}$ $K^{-1}$ |
| $1.6 \pm 0.1$ | $13.7 \pm 0.2$ | 2.6 | $11.1 \pm 0.6$ | $-17$ | $2.9 \pm 0.3$ | $21 \pm 1$ |

the distance of closest approach, the usual value of $5 \times 10^{-8}$ cm is used, one obtains, for the binding step involving the anion $L^-$, $K_{OS} = 1.6$ $M^{-1}$ ($T = 25°$, $I = 0.2$ M) and $k_2* = 5.4 \times 10^4$ $s^{-1}$. The good agreement between $k_2*$ and $Sk_{H_2O}$ indicates that $Ni^{2+}$ reacts with the anion of BHA "normally"; namely, the rate-determining step of the binding process is the loss of the first water molecule from $Ni(H_2O)_6$, $L^+$ (the ion pair) to give the monodentate complex, while the subsequent chelation step is relatively fast. This behavior implies that, in water, $L^-$ should be present mainly in the *Z* form, the only one capable of undergoing chelate formation, and this form should be the majority. Otherwise, the value of $k_2*$ would be less than that of $Sk_{H_2O}$ by a factor $K_{ZE}/(1 + K_{ZE})$. Assume, for instance, that the *Z* form is only 10% of the total ligand; then it would follow that $K_{ZE} = 0.11$ and $k_2* = Sk_{H_2O}\,K_{ZE}/(1 + K_{ZE}) = 2.3 \times 10^3$ $s^{-1}$, which is about twenty times less than the found value. The results also indicate that, in water, the rate of the process $E \rightleftharpoons Z$ is fast compared to complex formation. If this were not the case, $1/\tau$ would display an inverse dependence on $C_M$, contrary to the experiments. The chelation process requires that the *Z* form should be O deprotonated. This does not exclude N deprotonation. However, the N anions can be partially converted to O anions by a fast, buffer-assisted proton transfer from oxygen to nitrogen.

Concerning Ni(II) binding to HL, it turns out that $k_1* = 4.9 \times 10^3$ $s^{-1}$, 1 order of magnitude lower than $k_2*$ and much lower than $k_{H_2O}$. One could not ascribe this noticeable reduction of rate ($k_1*/k_2* = 0.09$) to a slow ring-closure step because this process was found to be fast in the reaction with $L^-$. Also, it could be argued that the rate reduction could be ascribed to the above-mentioned uncertainty (200−300%) on the $K_{OS,1}$ and $K_{OS,2}$ values. It should, however, be noted that even if the uncertainty in the absolute $K_{OS}$ values is large, this is not the case for the ratio $K_{OS,1}/K_{OS,2}$ because, for similar ligands, the distance of the reactants in the outersphere complex does not depend on the ligand charge. As a consequence, the relatively large difference between $k_1*$ and $k_2*$ could not be ascribed to improper values of $K_{OS}$. An alternative mechanism, based on slow HL and MHL deprotonation, has been proposed to explain the reduced rate of binding of the neutral acetohydroxamic acid to $Ni^{2+}$, $Co^{2+}$, and $Zn^{2+}$.[18] This mechanism does not apply to our system because, in $3 \times 10^{-3}$ M sodium cacodylate buffer ($HB/B^-$), the vertical steps shown in Scheme 5 are very fast. In particular, the rate constant for the $MHL^{2+} + B^- \rightarrow ML^+ + HB$ step is diffusion-controlled because this process

**Scheme 6**

$$HL_E \rightleftharpoons HL_Z$$

$$M + HL_Z \rightleftharpoons MHL$$

is thermodynamically favored ($pK_{HB} = 6.19$[33] and $pK_{MHL} = 4.81$).

The reaction mechanism where the first step is rate-determining has been considered. This mechanism was proposed for the binding of $Cu^{2+}$ and $La^{3+}$ to *N*-methylacetohydroxamic acid.[34] If this were the case for our system, then the measured relaxation time should tend to level off at the highest $Ni^{2+}$ concentrations, contrary to the results shown in Figure 10. It could then be assumed that the $HL_E \rightleftharpoons HL_Z$ step in aqueous solution is faster than the complex formation step. Under these circumstances, it would result that $k_1 = (k'_1K_{EZ})/(1 + K_{EZ})$. One could evaluate $k'_1$ as $k'_1 = k_{H_2O}SK_{OS} = 6.8 \times 10^3$ $s^{-1}$, from which one obtains $K_{E-Z} = 0.4$. This result would indicate that, in water, the *E* form is the majority, in disagreement with the NMR results on *N*-methylacetohydroxamic ($K_{E-Z} = 3.5$)[4b] and acetohydroxamic acid ($K_{E-Z} = 32$).[3] The NMR data obtained in acetone could not be extrapolated in aqueous solution, but the above results also suggest that, for BHA, the *Z* form is favored (because of the intramolecular O−H−O hydrogen bonding). Assuming that the *Z* form is prevailing in water, the complex formation rate reduction with respect to the expected value could be ascribed to the additional energy barrier due to the hydrogen bond, which blocks the reaction site.[35]

## Conclusions

The results of this study indicate that BHA adopts the amide structure in all of the investigated media (gas phase, acetone, and water). This structure displays *Z* (cis) and *E* (trans) isomerism. Ab initio calculations and kinetic measurements suggest that the *Z* form is favored in the gas phase and water, whereas NMR measurements indicate that, in acetone, the *E* form is the majority, the population ratio being $[E]/[Z] = 75:25$. In acetone, BHA dimerizes at low temperatures, giving *E*−*E*, *Z*−*Z*, and *E*−*Z* aggregates, which dissociate to the corresponding monomers in the presence of even minute amounts of water. The deprotonation site of BHA also depends on the nature of the medium. The theoretical calculations suggest that, in the gas phase, the deprotonation of the nitrogen atom is favored, the NMR results indicating that N and O deprotonations of the hydroxamate group occur to similar extents. The kinetic

(33) Diebler, H.; Secco, F.; Venturini, M. *J. Phys. Chem.* **1984**, *88*, 4229−4232.
(34) Biruš, M; Gabričević, M; Kronja, O. *Inorg. Chem*. **1999**, *38*, 4064−4069.

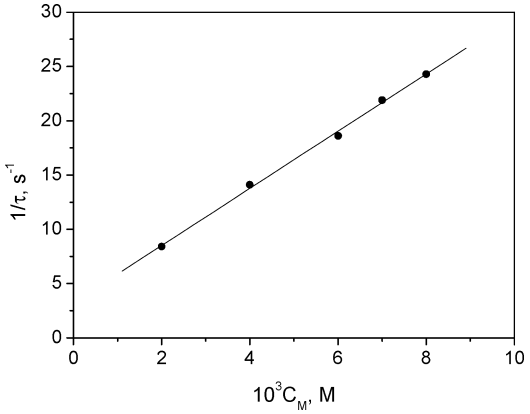


**Figure 10.** Dependence of the reciprocal relaxation time on the metal ion concentration for the BHA/Ni(II) system in aqueous solution. $[H^+] = 1.7 \times 10^{-7}$ M, $I = 0.2$ M, and $T = 25$ °C.

experiments performed in aqueous solution are not able to reveal which kind of deprotonation process occurs in water. However, the magnitude of the rate constant of the step of $Ni^{2+}$ binding to deprotonated BHA suggests that considerable amounts of the O anion should be present; this could be formed either by O deprotonation or by N deprotonation followed by a fast, buffer-assisted proton migration from O to N of the *Z* form. The extent of rate reduction of the binding of $Ni^{2+}$ to neutral BHA is interpreted assuming that the *Z* isomer, which prevails in water, is present mainly in a closed (hydrogen-bonded) structure, which should be open (with an energy penalty) in order for the metal binding to occur.

## Computational and Experimental Section

**Computational Details.** Computations were performed by an ORIGIN 3800 IRIX64 processor computer at the RHF/cc-pVDZ level. The most stable neutral and anionic forms were refined with density functional theory calculations (B3LYP/AUG-cc-pVDZ) to correct the electronic correlation without large computational expenses. To refine calculations, basis sets containing diffuse functions (AUG-cc-pVDZ) were employed, which are more accurate for describing anionic species. All of the calculations have been performed with the Gaussian 98 package.[36] Solvent effects in water and acetone were evaluated by means of the PCM method,[22,23] in which the solvent is regarded as a continuum dielectric characterized by a constant permittivity. The dielectric constants of acetone and water were set to 20.59 and 78.45 at 298.15K, respectively.

**Chemicals.** All chemicals were analytical grade (Fluka or Merck). BHA was recrystallized from water, and to minimize the residual trace water, it was kept under a vacuum for 48 h. The NMR solvent used, acetone-$d_6$ SDS (>99.8%), was purified as previously described;[2] however, traces of water from the solute could not be removed. The solubility of BHA in water is too low

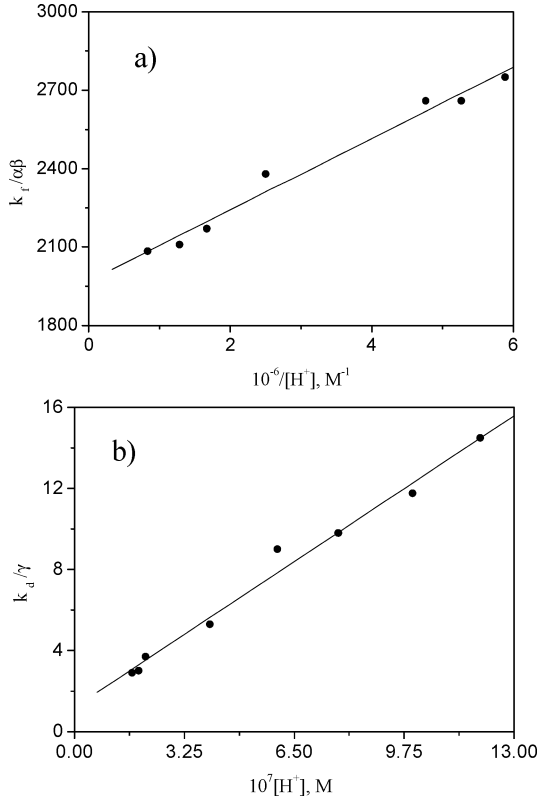


**Figure 11.** Dependence of the apparent kinetic constants on the medium's acidity for the BHA/Ni(II) system in aqueous solution. $I = 0.2$ M and $T = 25$ °C: (a) complex formation; (b) complex dissociation.

to provide reliable NMR signals. BHA is soluble in methanol and ethanol and in their mixtures with water, but the strong proton exchange removes the singlets from the spectrum.

**Methods.** The NMR measurements were performed with a Unity Inova Varian 400 instrument at 9.4 T (operating at 399.941 MHz). The spectra were recorded in acetone over the −80 to +40 °C temperature range using a spectral window of 15 ppm. The acquisition time was 13.2 $\mu$s, and a pulse angle of $\pi/2$ was employed. The solvent signal was used as a reference. The exchange rate constants were evaluated with the gNMR program (version 4.1), which is capable of simulating one-dimensional NMR spectra. The deconvolution of spectral signals was analyzed with the program GRAMS/AI 7.01 Thermo Galactic, 2002.

The $^1H-^1H$ NOESY spectra at −80 °C were recorded under the following conditions: relaxation delay, 1.000 s; mixing, 0.500 s; acquisition time, 0.236 s; 1D and 2D widths, 4333.5 Hz; 16 repetitions; 2 × 200 increments; observe 1H; 399.940 982 8 MHz. Data processing: Gauss apodization 0.109 s. F1 data processing: Gauss apodization, 0.043 s; FT size, 2048 × 2048. The $^1H-^1H$ COSY spectra were recorded under the following conditions: relaxation delay, 1.000 sec; acquisition time, 0.241 s; width, 4242.2 Hz; 4 repetitions; 256 increments; observe, 1H; 399.940 982 8 MHz. Data processing: sq sine bell, 0.030 s; FT size, 2048 × 2048.

The hydrogen ion concentration of solutions with $[H^+] \leq 0.01$ M were determined by pH measurements with a PHM 84 Radiometer Copenhagen or by a PHM Titrino DMS instrument. A combined glass electrode was used after the usual KCl bridge was replaced by 3 M NaCl to avoid the precipitation of $KClO_4$. The electrode was calibrated according to a procedure described elsewhere, which enables the conversion of the pH meter output into $-\log [H^+]$ values.[3] Absorption titrations were performed on a

(35) Mentasti, E.; Secco, F.; Venturini, M. *Inorg. Chem.* **1980**, *19*, 3528−3531.

(36) *Gaussian 94*, revision A.1; Frisch, M. J., Trucks, G. W., Schlegel, H. B., Gill, P. M. W., Johnson, B. G., Robb, M. A., Cheeseman, J. R., Keith, T. A., Petersson, G. A., Mongomery, J. A., Raghavachari, K., Al-Laham, M. A., Zakrzewski, V. G., Ortiz, J. V., Foresman, J. B., Cioslowsky, J., Stefanov, B. B., Nanayakkara, A., Challacombe, M., Peng, C. Y., Ayala, P. Y., Chem, W., Wong, M. W., Andres, J. L., Repogle, E. S., Gomberts, R., Martin, R. L., Fox, D. J., Binkley, J. S., Defrees, D. J., Baker, J., Steward, J. J. P., Head-Gordon, M., Gonzalez, C., Pople, J. A., Eds.; Gaussian, Inc.: Pittsburgh, PA, 1995.

Perkin-Elmer Lambda 17 double-beam spectrophotometer and on a HP 8453 diode array spectrophotometer equipped with a HP 89090A Peltier accessory to control the temperature. Experiments were performed at 15, 25, 35, 45, and 55 °C (± 0.1) because BHA undergoes hydrolysis above 55 °C at pH 8. Increasing amounts of the titrant were added by a microsyringe to a solution of BHA already thermostated in the measuring cell and kept under a nitrogen atmosphere. The spectra were recorded under a nitrogen atmosphere after each addition of the titrant and corrected for the dilution. The reversibility of the acid−base process was checked frequently.

The kinetic experiments were performed at 260 nm using a stopped-flow apparatus constructed in our laboratory. A Hi-Tech SF-61 mixing unit was coupled to a spectrophotometric line through two optical guides. The UV radiation produced by a Hamamatsu L248102 "quiet" lamp was passed through a Bausch and Lomb 338875 high-intensity monochromator and then split into two beams. The reference beam was sent directly to a 1P28 photomultiplier; the measuring beam was sent through a quartz optical-guide to the observation chamber and then through a second optical guide to the 1P28 measuring photomultiplier. The outputs of the two photomultipliers were balanced before each shot. The signal revealing the course of the reaction was sent to a Tektronix TDS210 oscilloscope equipped with a digital storage unit capable of memorizing 2500 data points at a maximum sampling rate of 60 MHz. Finally, the acquired signal was transferred to a personal computer via a GPIB interface, using the wavestar 2.0 program, and analyzed by a nonlinear least-squares procedure.[37] The observed time constants were averaged over at least six repeated experiments, the maximum spread being within 10%. The medium's acidity and the ionic strength were kept constant at the desired values during each experiment.

**Acknowledgment.** Thanks are due to J. Delgado and A. Muñoz (Burgos University). This work was supported by MIUR (Italy) through COFIN 2002; Ministerio de Ciencia y Tecnología (Spain), Projects BQU 2002-01061 and AYA 2002-02117; Junta de Castilla y León (Spain), Project BU 26-02; and Junta de Comunidades de Castilla−La Mancha (Spain), Grant PAI-02-001.

**Supporting Information Available:** Parameters from ab initio calculations, NMR/NOESY spectra, and stopped-flow kinetic curves. This material is available free of charge via the Internet at http://pubs.acs.org.

IC049438G

(37) Provencher, S. W. *J. Phys. Chem*. **1976**, *64*, 2772−2777.